

# A note on the extensivity of the holographic entanglement entropy

JOSÉ L.F. BARBÓN AND CARLOS A. FUERTES

*Instituto de Física Teórica IFTE UAM/CSIC  
Facultad de Ciencias C-XVI*

*C.U. Cantoblanco, E-28049 Madrid, Spain*  
jose.barbon@uam.es, carlos.fuertes@uam.es

## Abstract

We consider situations where the *renormalized* geometric entropy, as defined by the AdS/CFT ansatz of Ryu and Takayanagi, shows extensive behavior in the volume of the entangled region. In general, any holographic geometry that is ‘capped’ in the infrared region is a candidate for extensivity provided the growth of minimal surfaces saturates at the capping region, and the induced metric at the ‘cap’ is non-degenerate. Extensivity is well-known to occur for highly thermalized states. In this note, we show that the holographic ansatz predicts the persistence of the extensivity down to vanishing temperature, for the particular case of conformal field theories in  $2+1$  dimensions with a magnetic field and/or electric charge condensates.

# 1 Introduction

A very interesting proposal for a holographic [1] computation of geometric (entanglement) entropy [2] in conformal field theories was put forward in [3] (see [4] for subsequent work). The proposed procedure bears a close similarity with the holographic calculation of Wilson and 't Hooft loops in gauge theories and applies strictly to a large- $N$ , strong coupling limit of the quantum field theories (QFT) in question.

In recent years, entanglement entropy has gradually emerged as a useful non-local order parameter to characterize new phases in strongly coupled systems at zero temperature (cf. for example [5]). It is therefore of great interest to parametrize the different types of qualitative behavior that can be identified from the AdS/CFT side. In this direction, the authors of [6] have made the interesting observation that the scaling of geometric entanglement entropy is a good order parameter of confinement in gauge theories that admit standard AdS-like duals (see also the earlier work of Ref. [7]). In particular they found that for regions of size bigger than the confining scale the renormalized entanglement entropy<sup>1</sup> suddenly becomes strictly proportional to the area of the region with a constant of proportionality *independent* of the size, unlike conformal field theories. In this paper, we follow this program, focusing on the property of *extensivity*, an admittedly *non generic* feature of geometric entropy in standard weak-coupling calculations at zero temperature.

In this note, we begin with a review of the holographic proposal of [3], emphasizing the natural emergence of the non-extensive ‘area law’ for the geometric entropy in models with conformal ultraviolet fixed points. It is then argued that extensivity of the renormalized finite entropy is quite a generic feature of the holographic models with a gapped spectrum. We discuss in some detail the conditions that ensure this behavior, and comment on the relation to the confinement property, making contact with the results of [6].

Finally, we focus on a particular model of especial interest, namely the case of conformal field theories (CFT) in  $2 + 1$  dimensions with a magnetic field and/or electric charge condensates, holographically represented by zero-temperature extremal black holes with finite horizon area in Anti-de Sitter space (AdS). The relevance of this system stems from the fact that the extensive law, characteristic of high-temperature states, does persist all the way down to zero temperature.

## 2 Review of the holographic ansatz

The starting point of the holographic proposal of [3] is the *replica trick* calculation of the entanglement entropy [9]. Consider a quantum field theory defined on a Hamiltonian spacetime of the form  $\mathbb{R} \times X_d$ , with  $X_d$  a  $d$ -dimensional spatial manifold. Given a general state  $\rho$  defined in terms of the Hamiltonian quantization on  $X_d$ , let  $A$  denote a  $d$ -dimensional region of  $X_d$ , with smooth boundary  $\partial A$ , and consider the inclusive density

---

<sup>1</sup>We understand by renormalized entanglement entropy the quantity obtained by subtracting the ultraviolet divergent term to the entanglement entropy. A more refined quantity is the *entropic C-function* [8] to which all our comments equally apply.

matrix obtained by tracing out degrees of freedom inside A;  $\rho_A = \text{Tr}_A \rho$ . The associated entanglement entropy can be computed as [9]

$$S_A = -\text{Tr} \rho_A \log \rho_A = -\frac{d}{dn} \Big|_{n=1} \text{Tr} (\rho_A)^n . \quad (1)$$

The path-integral representation of  $\text{Tr} (\rho_A)^n$  can be manipulated into a frustrated (Euclidean) partition function on a theory with  $n$  copies of the original QFT,

$$\text{Tr} (\rho_A)^n = \left\langle \mathbf{T}_{\partial A}^{(n)} \right\rangle_{\text{QFT}^{\otimes n}} , \quad (2)$$

where the twist operator  $\mathbf{T}_{\partial A}$  is defined by introducing the following boundary conditions in the path integral,

$$\Phi_i^{(+)} = \sum_{j=1}^n \Gamma_{ij} \Phi_j^{(-)} , \quad (3)$$

with  $\Gamma_{ij} = \delta_{i,j+1} + \delta_{n,1}$  identifying fields of consecutive copies across the set A. The superscripts  $(\pm)$  in (3) denote the ‘two sides’ of A, when embedded in the complete Euclidean manifold  $\mathbb{R} \times X_d$ . Alternatively, for any point  $P \in A$ ,  $\Phi^{(+)}(P)$  is obtained from  $\Phi^{(-)}(P)$  by transporting the field from the ‘lower side’ to the ‘upper side’ of A along a closed path of linking number one with the boundary  $\partial A$ . In particular, the construction shows that the twist operator in (2) is ‘instanton-like’, i.e. it is always sharply localized in the time direction.

The twist operator  $\mathbf{T}$  is locally supported on  $\partial A$ . The simplest particular case occurs in 1 + 1 dimensions, where the non-local twist operator is given by a *bilocal* product of two standard (local) twist operators, i.e. (2) is a two-point function. In 2 + 1 dimensions,  $\mathbf{T}$  is supported on a one-dimensional curve, just like standard Wilson and ’t Hooft loop operators. Taking inspiration from the case of Wilson loops, one’s natural guess for the ultraviolet contribution to (2) is

$$\left\langle \mathbf{T}_{\partial A}^{(n)} \right\rangle_{\text{UV}} \sim \exp (-\alpha_n \varepsilon^{1-d} |\partial A|) , \quad (4)$$

with  $\varepsilon$  a short-distance cutoff and  $|\partial A|$  the volume of  $\partial A$  in the metric of the spatial manifold  $X_d$ . Although all previous expressions hold in an arbitrary QFT in a formal sense, Eq. (4) assumes that  $\varepsilon^{-1}$  is taken beyond any mass scale in the theory, so that we are close to some ultraviolet (UV) fixed point. Since (2) is almost an  $n$ -fold product of partition functions, we expect  $\alpha_n/n$  to be finite in the  $n \rightarrow \infty$  limit. Furthermore, we know that  $\alpha_1 = 0$ , since the partition function is not ‘frustrated’ for  $n = 1$ . The resulting entanglement entropy has the form

$$S_A = \frac{d\alpha_n}{dn} \Big|_{n=1} \frac{|\partial A|}{\varepsilon^{d-1}} + \dots , \quad (5)$$

where the dots stand for less divergent terms, which will depend in general on the size and shape of A and any intrinsic mass scales of the QFT. In Eq. (5) we see the expected UV scaling of the geometric entropy, i.e. non-extensive behavior and ‘area law’ with respect to the entangled region [2].

## 2.1 AdS and area law

By direct analogy with the treatment of Wilson and 't Hooft loops in gauge theories, the authors of [3] propose to compute (2) in an AdS/CFT prescription involving a minimal hypersurface with boundary data given by  $\partial A$ . This procedure can be strictly justified for the particular case of two-dimensional conformal models, for then (2) becomes a two-point function of *local* conformal operators. More generally, we have the ansatz

$$\left\langle \mathbf{T}_{\partial A}^{(n)} \right\rangle_{\text{QFT}^{\otimes n}} \approx \exp(-c_n \text{Vol}(\bar{A})) , \quad (6)$$

where  $\bar{A}$  is the minimal  $d$ -dimensional hypersurface dropped inside the bulk of the AdS space, with boundary conditions  $\partial \bar{A} = \partial A$  at the UV boundary of AdS.  $\text{Vol}(\bar{A})$  stands for the volume of the hypersurface as induced from the ambient AdS metric. Computing the entropy via the replica-trick formula we find

$$S_A \approx \left. \frac{dc_n}{dn} \right|_{n=1} \text{Vol}(\bar{A}) = \frac{\text{Vol}(\bar{A})}{4G_{d+2}} , \quad (7)$$

where the precise coefficient is fixed in [3] by comparison with known standard results in two dimensions. Considering bulk spaces with AdS asymptotics near the boundary:

$$ds^2/R^2 \longrightarrow u^2 (d\tau^2 + d\vec{x}^2) + du^2/u^2 , \quad (8)$$

any minimal hypersurface  $\bar{A}$  with a boundary component at infinity is asymptotically perpendicular to the boundary, with a volume divergence at large  $u$  of the form

$$\frac{R^d u_\varepsilon^{d-1} |\partial A|}{4G_{d+2}} \propto N_{\text{eff}} \frac{|\partial A|}{\varepsilon^{d-1}} , \quad (9)$$

where  $u_\varepsilon = \varepsilon^{-1}$  and  $N_{\text{eff}} = R^d/G_{d+2}$  is the effective number of degrees of freedom of the conformal UV fixed point.<sup>2</sup> Hence, the holographic ansatz obtains the expected UV structure (4).

In addition to the UV asymptotics, one can determine a UV-finite part that is always present in the conformal approximation of (8), the renormalized entanglement entropy. To find this term, let us focus on a simple situation where  $X_d = \mathbb{R}^d$  and let  $A$  be the  $d$ -dimensional *strip*, i.e. the product of a finite interval of length  $\ell$  times an infinite hyperplane of codimension one in space:  $A = [-\ell/2, \ell/2] \times \mathbb{R}^{d-1}$ . By translational invariance on  $\mathbb{R}^{d-1}$  we know that the entropy will be extensive along these  $d-1$  dimensions. Furthermore, a rescaling of the boundary coordinates,  $\vec{x}$ , induces a rescaling of  $\ell$  which can be absorbed in a rescaling of  $u$  in (8) leaving the metric invariant. Hence, the induced

---

<sup>2</sup>For example, for models governed by a large- $N$  gauge theory we have  $N_{\text{eff}} \sim N^2$ . Other models, such as the theory on a stack of  $N$  M2-branes, have  $N_{\text{eff}} \sim N^{3/2}$ , whereas  $N_{\text{eff}} \sim N^3$  for a stack of  $N$  M5-branes.

volume of  $\bar{A}$  is invariant under these combined scalings and the finite part of the entropy must be of the form

$$C_A(\ell) = \ell \frac{d}{d\ell} S_A \propto N_{\text{eff}} \frac{|\mathbb{R}^{d-1}|}{\ell^{d-1}}, \quad (10)$$

where the factor of  $N_{\text{eff}}$  is ensured by dimensional analysis and the overall factor of  $G_{d+2}^{-1}$ . The quantity defined in (10), designed to remove the leading UV term, is also called the ‘entropic C-function’ [8]. Therefore, a form of ‘area law’ also holds at conformal fixed points, at the level of the renormalized entropy.

If the UV fixed point is associated to a holographic model of the form  $\text{AdS}_{d+2} \times K$ , with  $K$  some compact Einstein manifold of dimension  $d_K = D - d - 2$ , this extra structure only enters (7) through the Kaluza–Klein reduction of Newton’s constant  $G_{d+2}^{-1} = G_D^{-1} \text{Vol}(K)$ . Therefore, we can generalize the prescription to the higher-dimensional description via a minimal  $(D - 2)$ -dimensional hypersurface which wraps completely the internal manifold. The Kaluza–Klein ansatz also applies to warped products of AdS-like spaces and compact manifolds, where the radius of curvature of both factors has a non-trivial dependence on the holographic coordinate  $u$ . If  $R$  and  $G_{d+2}$  denote the asymptotic values of curvature radius and Newton’s constant, the ansatz (7) remains valid, ensuring UV asymptotics controlled by  $N_{\text{eff}} \sim R^d/G_{d+2}$  as before, but with modified behavior at the level of the renormalized entropy. Models arising from ten-dimensional string backgrounds are treated in the same way, provided we remember to use the Einstein-frame metric in the ten-dimensional set up before the Kaluza–Klein reduction.<sup>3</sup>

In order to fix the notation, let us consider  $(d + 2)$ -dimensional spaces with Einstein-frame metric

$$ds^2 = R^2 \alpha(u)^2 \left( \frac{\beta(u)^2}{h(u)} du^2 + d\vec{x}^2 + h(u) d\tau^2 \right), \quad (11)$$

which are assumed to asymptote  $\text{AdS}_{d+2}$  at  $u \rightarrow \infty$  with radius  $R$ , i.e. the background profile functions,  $\alpha(u)/u$ ,  $\beta(u)u^2$  and  $h(u)$  all approach unity at infinity. More general situations, where the model has no smooth UV fixed point, can be dealt with by defining a running number of degrees of freedom  $N_{\text{eff}}(u)$ . We include the Lorentz-violating profile function  $h(u)$  in order to extend the analysis to black-hole spacetimes.

One can further reduce the expression (7) for the particular situation of the strip:  $A(\ell) = [-\ell/2, \ell/2] \times \mathbb{R}^{d-1}$ , leading to a bulk hypersurface  $\bar{A}$  called the ‘straight belt’ in [3]. The ‘longitudinal’ entropy density along the strip,  $s_A = S_A/|\mathbb{R}^{d-1}|$ , is given by

$$s_A = \frac{R^d}{4G_{d+2}} \int_{-\ell/2}^{\ell/2} dx \gamma(u) \sqrt{1 + \frac{(\beta(u)\partial_x u)^2}{h(u)}}, \quad (12)$$

with  $\gamma(u) \equiv \alpha(u)^d$ . This functional defines a variational problem for the profile  $u(x)$ , which is parametrized by the radial position  $u_*$  of the turning point  $\partial_x u = 0$ . The functional relation between  $\ell$  and  $u_*$  is given by

$$\ell(u_*) = 2\gamma(u_*) \int_{u_*}^{\infty} \frac{du \beta(u)}{\sqrt{h(u) (\gamma(u)^2 - \gamma(u_*)^2)}}. \quad (13)$$

---

<sup>3</sup>The difference between both frames amounts to a factor of  $\exp(-2\phi)$  in the induced volume 8-form.

Notice, however, that the minimizing hypersurface might not be a smooth one, in which case (13) ceases to apply.

The law  $\ell(u_*) \sim 1/u_*$ , characteristic of the conformal case, can be readily obtained by a heuristic argument. Let us model the surface  $\bar{A}$  as the union of two components. The first component is a cylinder extending from radial coordinate  $u_m$  up to  $u_\varepsilon$ , and subtending a strip of length  $\ell$  in the boundary metric. The second component is the ‘cap’ at  $u = u_m$ . The entropy functional is obtained by adding the volumes of each component. Factoring out the longitudinal volume of the strip we find

$$s_A(u_m) \sim N_{\text{eff}} (u_\varepsilon^{d-1} - u_m^{d-1}) + N_{\text{eff}} u_m^d \ell ,$$

with the first term coming from the cylinder and the second one from the cap at  $u = u_m$ . Minimizing with respect to  $u_m$  we find an optimal turning point satisfying  $(d-1)u_*^{d-2} - \ell d u_*^{d-1} = 0$ , which yields the desired relation  $\ell u_* \sim 1$ .

### 3 Extensivity and infrared walls

In a model that combines a UV fixed point and an intrinsic energy scale  $M$ , the holographic dual geometry will remain approximately AdS until we reach radial coordinates of order  $u_0 \sim M$ , and the form (10) is a good approximation as long as  $\ell M \ll 1$ . A typical instance of nontrivial infrared (IR) behavior is that the radial coordinate ‘terminates’ at  $u_0 = M$ , either because of the existence of some sort of sharp wall, a ‘repulsive’ singularity, or perhaps a vanishing cycle along the rest of the dimensions. In this section we study the different types of qualitative behavior to be expected when the turning point  $u_*$  approaches the wall position  $u_0$ . By the conformal UV/IR relation,  $\ell u_* \sim 1$ , this will occur roughly around  $\ell \sim 1/M$ .

#### 3.1 IR wall avatars

The precise functional dependence  $\ell(u_*)$  is specified in Eq. (13), which we may rewrite as

$$\ell = \int_1^\infty \frac{dx \zeta(x)}{\sqrt{x^2 - 1}} , \tag{14}$$

where we have made a change of variables  $x = \gamma(u)/\gamma(u_*)$  and we have defined the function  $\zeta(x)$  by

$$\zeta(x) = 2 \frac{\gamma(1) \beta(x)}{\gamma'(x) \sqrt{h(x)}} , \tag{15}$$

where  $\gamma' \equiv d\gamma/du$ . The turning point  $u = u_*$  lies at  $x = 1$  in the new variables, so that  $\gamma(1) = \gamma(u_*)$ , and the wall sits at some  $x = x_0 < 1$ . In the following, we use the notation  $\gamma(u_0) \equiv \gamma_0$  and  $\gamma'(u_0) \equiv \gamma'_0$ . There are three basic types of qualitative behavior as the turning point of *smooth* surfaces approaches the wall,  $x_0 \rightarrow 1$ , depending on whether  $\ell$  diverges, approaches a constant value, or vanishes in this limit. These three alternatives

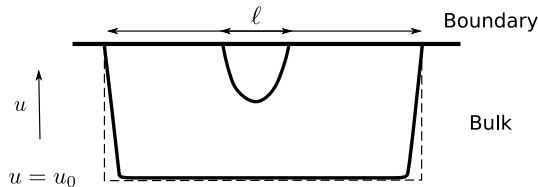


**Figure 1:** Schematic plot of the typical configuration of a smooth minimal surface that gives us the entanglement entropy in the presence of infrared walls. Close to the position of the infrared wall, the surface prefers to lean on it, giving an extensive contribution to the entropy. We also show the ‘capped cylinder’ in dashed lines, which becomes a better and better approximation to the minimal surface as  $\ell \rightarrow \infty$ .

can be translated into corresponding qualitative properties of the background, through the structure of the function  $\zeta(x)$  in the vicinity of the wall  $x \sim x_0$ .

In our analysis, we shall adopt some technical assumptions derived from experience with concrete examples of holographic duals. First, we assume that  $\beta(u)$  is smooth and positive for all  $u \geq u_0$ . The Schwarzschild-like factor  $h(u)$  will be positive as well, except for a possible single zero at  $u = u_0$ . Finally, the warp factor  $\gamma(u)$  is taken to be positive and monotonically increasing for all  $u > u_0$ , but we allow for the possibility that it may vanish right at the wall position. Within these technical assumptions, the only possible singularity structure of  $\zeta(x)$  is either a pole at  $x = x_0$ , coming from a zero of the warp-factor derivative,  $\gamma'(u_0) = 0$ , or a square root singularity  $\zeta(x) \sim (x - x_0)^{-1/2}$ , coming from a regular black-hole horizon,  $h(u_0) = 0$ .

Since we are assuming that the model has an UV fixed point, we know that the contribution of large values of  $x$  to (14) is well approximated by the conformal law  $\ell_{\text{high}} \sim 1/u_0 \sim 1/M$ . Then, if  $\zeta(x)$  is smooth in the vicinity of  $x = 1$  we have a finite  $\ell \propto 1/u_0$  as  $u_* \rightarrow u_0$ , perhaps decorated with some numerical factors involving dimensionless parameters of the background. A vanishing  $\ell$  in the wall limit can only result from a vanishing warp factor  $\gamma_0 = 0$ .

Finally, when  $\zeta(x)$  diverges as  $(x - x_0)^{-1/2}$  or faster, we have  $\ell \rightarrow \infty$  as  $x_0 \rightarrow 1$ . Then we say that the smooth surface *saturates* at the wall. In this case we have the situation depicted in Fig. 1, where a smooth surface asymptotically rests over the wall, forming a cap that is smoothly joined by an almost cylindrical surface of section  $\partial A$ , reaching out to the boundary. In the limit of very large  $\ell$  the resulting entropy is very well approximated by that of the ‘capped cylinder’, obtained by adjoining a ‘cap’  $u_0 \times A$  to the cylinder  $[u_0, \infty] \times \partial A$  (in the case of the strip, the cylinder is just given by the two straight  $[u_0, \infty] \times \mathbb{R}^{d-1}$  panels, suspended a distance  $\ell$  apart).

We are now ready to detail the casuistics of different types of walls regarding their saturation properties.

### 3.1.1 Soft walls

These walls are characterized by a local minimum of the warp factor,  $\gamma'_0 = 0$ , with

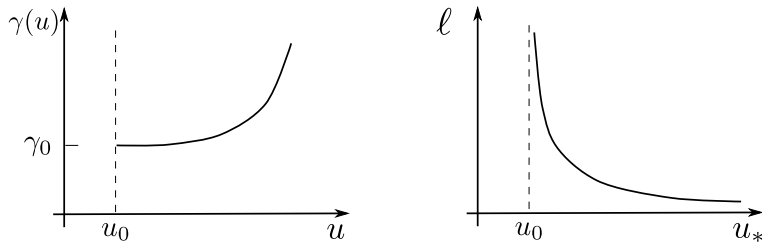


**Figure 2:** Qualitative behavior of the warp factor near a soft wall, with  $\gamma'_0 = 0$  and  $\gamma_0 > 0$ . On the right, the corresponding UV/IR relation with saturation,  $\ell \rightarrow \infty$ , at the wall.

$\gamma_0 > 0$  (we set  $h(u) = 1$  for simplicity). Then  $\zeta(x) \sim (x - x_0)^{-1}$  and the smooth surfaces saturate (cf. Fig 2),  $\ell \rightarrow \infty$  as  $u_* \rightarrow u_0$ . We call these walls ‘soft’ because the function  $\gamma(x)$  usually extends for  $x < x_0$ , albeit with negative derivative. Static masses feel a repulsive gravitational force that prevents physical probes from reaching far into the  $x < x_0$  region. Particular examples include the confinement models of [10] based on backgrounds with naked singularities. Hence, these models are usually regarded as formal qualitative tools at best.

### 3.1.2 Hard walls

These walls are defined by  $\gamma_0, \gamma'_0 > 0$ , i.e. they behave formally as the ‘sharp cutoff’ regularization of a simple AdS background and are commonly used in phenomenological discussions of AdS/QCD, as in [11]. In a formal sense, they can be obtained as the ‘stiff’ limit of the soft walls in the previous subsection, that is to say the limit in which the minimum of  $\gamma(u)$  at  $u = u_0$  is made sharper and sharper.

Regarding the entanglement entropy, the most striking property of these walls is a UV/IR relation  $\ell(u_*)$  with a maximal value of  $\ell$  (cf. Fig. 3). Indeed, for  $\ell > \ell_{\max}$  the minimizing surface is not smooth. By explicit inspection, we can see that the cylinder  $[u_0, \infty) \times \partial A$ , with a cap  $u_0 \times A$  right at the wall is a minimal surface (any perturbation takes an element of the surface to larger  $u$ , so that it increases the induced volume). Notice that this surface is not smooth because it has sharp edges at the juncture between the cap and the cylinder, but it is clearly connected and has the same topology as the smooth surfaces that extremize the problem for  $\ell < \ell_{\max}$ .

### 3.1.3 Resolved walls

These walls are characterized by a vanishing warp factor,  $\gamma_0 = 0$ , at the location of the wall. As a result, the function  $\ell(u_*)$  vanishes as  $u_* \rightarrow u_0$ . As depicted in Fig. 4 there is again a maximal  $\ell_{\max}$  but now there are two smooth extremal surfaces for any  $\ell < \ell_{\max}$ . This is the case studied at length in the examples of Ref. [6]. It corresponds to most well defined models of confinement, in which the vanishing induced metric  $\gamma_0 = 0$  arises from a vanishing cycle in some extra dimension, in such a way that the higher-dimensional metric



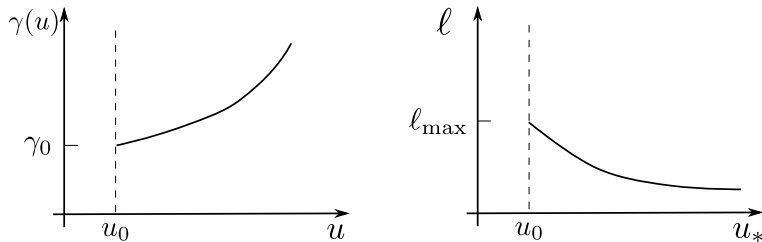


**Figure 3:** Qualitative behavior of the warp factor near a hard wall, with  $\gamma'_0 > 0$  and  $\gamma_0 > 0$ . On the right, the corresponding UV/IR relation with a maximal value of  $\ell$ .

is completely smooth at  $u = u_0$ . For this reason we refer to these walls as ‘resolved’ by the higher-dimensional uplifting.

In addition to the mentioned examples studied in [6], there is a different type of model that belongs to this class, namely that of spherical distributions of D-branes in the Coulomb branch of  $N = 4$  super Yang–Mills theory (cf. [12]). The dual supergravity configuration consists of a standard  $\text{AdS}_5 \times \text{S}^5$  background for  $u > M$ , matched with a flat ten-dimensional metric inside the sphere at  $u = M$ , where  $M$  is the mass scale set by the Higgs mechanism in the Coulomb branch. The hypersurface entering the entropy ansatz wraps the  $\text{S}^5$  spheres, which remain of constant volume for all  $u > M$  but shrink to zero size as a standard angular sphere in polar coordinates for  $u < M$ . Since the five-dimensional warp factor  $\gamma(u)$  is proportional to the volume of the internal manifold at fixed  $u$ , we find ourselves in the qualitative situation of Fig. 4.

Among the two solutions for each  $\ell < \ell_{\text{max}}$ , the standard minimal embeddings correspond to the solution with the larger value of  $u$ , whereas the branch of solutions with  $\ell \rightarrow 0$  as  $u \rightarrow u_0$  corresponds to locally unstable surfaces. The absence of stable minimal surfaces for  $\ell > \ell_{\text{max}}$  makes this case similar to that of the hard wall, and the problem is resolved in the same fashion. Namely, the minimal surface at very large  $\ell$  is not smooth, consisting of the capped cylinder lying right at the wall.<sup>4</sup> A crucial difference with respect to the hard wall case is that  $\gamma_0 = 0$  and now the induced volume of the cap is not just minimal, but in fact it vanishes. Hence, the contribution of the minimal surface to the entropy is just given by the cylindrical portion, which was referred to in [6] as the ‘disconnected surface’, in the particular case of the strip.

It is important to stress, however, that the minimal surface with degenerate cap is just a member of a continuous set of surfaces with standard topology and with induced volume arbitrarily close to the minimal one. For this reason we do not think that the picture of a ‘disconnected surface’ is relevant or appropriate in general, despite the fact that it gives the same answer as the capped cylinder for the particular case of these walls (more on this in a subsequent section).

---

<sup>4</sup>As shown in [6] the capped cylinder remains the absolute minimum down to  $\ell_c$ , a critical length of order  $\ell_{\text{max}}$ , albeit somewhat smaller.

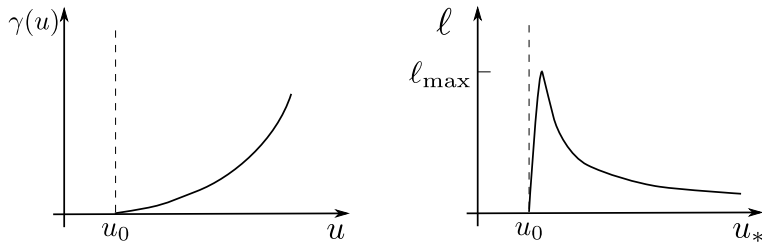


**Figure 4:** Qualitative behavior of the warp factor near a resolved wall, with  $\gamma'_0 > 0$  and  $\gamma_0 > 0$ . On the right, the corresponding UV/IR relation with a maximal value of  $\ell$  and two smooth extremal surfaces for each  $\ell < \ell_{\max}$ .

### 3.1.4 Thermal walls

Finally, the remaining case with a clear physical interpretation is that of a black hole horizon,  $h(u_0) = 0$ , corresponding to a plasma phase in the dual theory on the boundary. A regular (non-extremal) horizon will have  $h'(u_0) \neq 0$  and the effective function diverges as  $\zeta(x) \sim (x - x_0)^{-1/2}$  in the vicinity of the wall. This translates into a logarithmically divergent  $\ell$  in the limit  $u_* \rightarrow u_0$ , as defined by (14). In other words, we have saturation by smooth surfaces and a behavior qualitatively similar to that of the soft walls.

The full Euclidean metric (11) of the black hole backgrounds is smooth at the wall, since the compact thermal cycle with the inverse temperature identification  $\tau \equiv \tau + \beta$ , attains vanishing size at  $u = u_0$  in a smooth way. In this sense, this metric is similar to the higher-dimensional versions of the metric in the case of the resolved walls, discussed in the previous subsection. It is very important, however, to distinguish the two situations by recalling that the embedded surface  $\bar{A}$  is *always* localized in the  $\tau$  direction, so that the vanishing thermal cycle does not translate in a vanishing induced metric at the wall, i.e. we still have  $\gamma_0 > 0$  in this case. Conversely, the vanishing cycles in the examples of the previous subsection are being wrapped by the minimal surface, and do contribute to the vanishing of  $\gamma_0$  there.

## 3.2 Extensivity of the entropy

We conclude that in all cases the minimal surfaces effectively saturate at the wall. In some cases the saturating surface is smooth and well described by Eq. (14), whereas in some others the minimal surface is not smooth, given by the ‘capped cylinder’ at the wall. In either case, the entropy is well approximated by that of the capped cylinder, and in the cases of non-smooth minimal surfaces, it is exactly given (in the classical limit) by the volume of the capped cylinder. In fact, we may carry the complete discussion at a qualitative level in terms of a restricted family of surfaces, corresponding to cylinders of base  $\partial A$  with a cap at some  $u = u_m \geq u_0$ . The resulting entropy takes the form

$$S(u_m) = \frac{1}{4} N_{\text{eff}} \left[ |A| \alpha(u_m)^d + |\partial A| \int_{u_m}^{u_\epsilon} \frac{du}{\sqrt{h(u)}} \beta(u) \alpha(u)^d \right], \quad (16)$$

where the first term is the contribution of the cap at  $u = u_m$  and the second term corresponds to the cylinder extending from  $u = u_m$  up to the cutoff scale  $u = u_\epsilon$ . Recall that  $|A|$  and  $|\partial A|$  denote the volumes of  $A$  and its boundary in the field-theory metric. For the case of the strip  $2|A| = \ell|\partial A|$ . Taking the first derivative we find

$$\frac{dS}{du_m} = \frac{N_{\text{eff}}}{8} |\partial A| \left[ \ell d\gamma'(u_m) - 2 \frac{\beta(u_m)\gamma(u_m)}{\sqrt{h(u_m)}} \right], \quad (17)$$

where we have made use of  $\gamma(u) \equiv \alpha(u)^d$ . Furthermore, equating it to zero fixes  $u_m = u_*$  and we obtain the UV/IR relation in this approximation,

$$\ell(u_*) = \frac{2}{d} \frac{\beta(u_*)}{\sqrt{h(u_*)}} \frac{\gamma(u_*)}{\gamma'(u_*)}, \quad (18)$$

Eq. (18) shows all the qualitative features discussed previously on the basis of (14). In particular, we see that saturation, i.e.  $\ell(u_* \rightarrow u_0) \rightarrow \infty$  occurs whenever  $h(u_0) = 0$  or  $\gamma'(u_0) = 0$ , whereas  $\gamma(u_0) = 0$  ensures that there is a branch of solutions with  $\ell \rightarrow 0$  in the wall limit. Eq. (17) also shows that for resolved walls and hard walls with  $\gamma'_0 > 0$ , the entropy functional at fixed and large  $\ell$  satisfies  $dS/du_m > 0$  at  $u_m = u_0$ , so that the entropy is locally minimized by the capped cylinder at  $u_m = u_* = u_0$  provided  $\ell$  is large enough.

Hence, the entropy at very large  $\ell$  is well approximated by the induced volume of the capped-cylinder in all cases. The contribution from the cylinder contains the cutoff dependence and it is proportional to  $|\partial A|$ , i.e. it gives an area law. On the other hand, at large  $\ell$  it is asymptotically independent of  $\ell$ , so that it drops from the calculation of  $C_A(\ell)$ . The remaining finite term is the volume of the cap at  $u_* \approx u_0 = M$ , appropriately redshifted to that radial position, i.e.

$$S_{\text{cap}} \approx \frac{R^d \gamma_0 |A|}{4G_{d+2}}. \quad (19)$$

For a model asymptotic to AdS with curvature radius  $R$ , we can multiply and divide by  $(u_0)^d$  to obtain the extensive law

$$C_A(\ell) \approx S_{\text{cap}} \propto \eta_M N_{\text{eff}} M^d |A|, \quad (20)$$

with  $N_{\text{eff}}$  the effective number of degrees of freedom at the UV fixed point CFT and  $M = u_0$ , the value of the capping coordinate, determining the scale of the mass gap. The new parameter

$$\eta_M = \frac{\gamma_0}{(u_0)^d} \quad (21)$$

keeps track of the ‘flow’ of relevant parameters from the UV fixed point at  $u = \infty$  down to the IR mass scale  $u_0 = M$ . For example, for a model obtained by Kaluza–Klein reduction on some internal manifold  $K$ , we have

$$\eta_M = \frac{\text{Vol}(K_0)}{\text{Vol}(K_\infty)}, \quad (22)$$

where all volumes must be computed in Einstein-frame conventions, in the case of string backgrounds. In fact, we could define an effective ‘infrared’ number of degrees of freedom by the product  $N_{\text{eff},0} = \eta_M N_{\text{eff}}$ .

In many situations the flow parameter  $\eta_M$  is not qualitatively important. This is for example the case of black-hole backgrounds, with a dual interpretation in terms of thermal states of the QFT. In general  $\gamma_0 \neq 0$  at such a black hole horizon, and we obtain an extensive component of the entropy, in accordance with general expectations (c.f. [3])

$$S_A(T) \propto N_{\text{eff}} T^d |A| , \quad (23)$$

where  $u_0 \sim T$  for a large-temperature black hole in AdS. In the next section we introduce a very interesting system in which magnetic fields or charge condensates are capable of supporting a zero-temperature horizon with the formal properties of a thermal wall, namely supporting a nontrivial extensive law for the entanglement entropy.

Finally, the most notable exception to the extensive behavior is the case of resolved walls [6], with  $\gamma_0 = 0$ , which automatically yield  $\eta_M = 0$  by the vanishing of  $\text{Vol}(K_0)$  in (22).

### 3.2.1 The role of disconnected surfaces

We have stressed that the ‘disconnected surfaces’ invoked in [6] are in fact standard connected surfaces in which the ‘endcap’ contributes zero volume due to the degenerate induced metric at the wall.<sup>5</sup> Indeed, there is a continuous family of surfaces of standard topology that approximate arbitrarily well the volume of the so-called disconnected surface. Exactly the same situation occurs in the two-point function of Polyakov loops, using in that case the vanishing circle Euclidean black hole backgrounds (cf. for example the discussion in [13]).<sup>6</sup>

Invoking disconnected surfaces has the additional problem that they would naturally minimize the large  $\ell$  entropy in the presence of thermal walls, a situation in which we would lose the understanding of the extensivity of thermal entanglement entropy. We believe it more likely that disconnected surfaces are related to a different observable, namely the so-called *mutual information* (cf. for example [14] for a discussion of its properties and uses in quantum information). Mutual information between a bipartite partition of a system is defined as

$$I[A, B] \equiv S_A + S_B - S_{A \cup B} , \quad (24)$$

where the last term is the total von Neumann entropy of the whole system, and it vanishes for a pure state. On the other hand, for a thermal state the extensive terms cancel out of (24) and one is left with the area-law terms sensitive to the UV cutoff. Applying this prescription to the holographic ansatz in a black hole background one finds that the ‘caps’

---

<sup>5</sup>The term ‘disconnected surface’ strictly refers to the case of the strip, in which  $\partial A$  is the union of two  $\mathbb{R}^{d-1}$  planes. More generally, the ‘disconnected surface’ is regarded as the cylinder  $[u_0, \infty] \times \partial A$ .

<sup>6</sup>We stress once more that the surfaces computing entanglement entropy are always orthogonal to thermal circles, somewhat like *spatial* Wilson lines and strictly *unlike* timelike Wilson lines, also known as Polyakov lines.

in the saturation surfaces are subtracted out by the standard Bekenstein–Hawking entropy and what remains is twice the volume of the uncapped cylinder, scaling with an area law. This prediction is in agreement with the work of Ref. [15] where they demonstrate for lattice systems that the mutual information follows an area law. In this respect we propose to reinterpret the work in [16] as a calculation of the mutual information rather than the strict entanglement entropy at finite temperature.

### 3.2.2 Phase transitions

In the previous subsections we have discussed the different qualitative possibilities corresponding to different types of walls. With little more effort one can extend the analysis further and consider combined situations, where for instance a soft wall, with  $\gamma'_0 = 0$ , develops a degenerate metric at the wall position,  $\gamma_0 \rightarrow 0$ . In this case, one must study the relative rates at work, and concludes that the behavior of the prefactor  $\gamma(1)$  dominates, producing a situation akin to that of resolved walls.

Another interesting complication is the consideration of systems with IR walls *and* finite temperature. In this case one must compare the competing effects of the warp factor  $\gamma(u)$  *versus* the Schwarzschild factor  $h(u)$ . One must also consider phase transitions of the background, or Hawking–Page type. Roughly speaking the dominating background at a given temperature is the one with the largest value of the wall coordinate (up to transient effects that depend on the precise value of the free energies). For  $T \ll M$  the system is characterized by a zero-temperature wall and  $h(u) = 1$  (the ‘confined phase’), whereas for  $T \gg M$  the system is always in the plasma phase, and the relevant wall is the thermal one, determined by the zero of  $h(u_0) = 0$ .

We may then consider the behavior of the function  $s_A(\ell, T, M)$ . For  $\ell^{-1} \gg T, M$  the entanglement entropy shows conformal behavior. On the other hand, for  $\ell^{-1} < \max(T, M)$  the minimal surface will be well-approximated by the capped cylinder, and the finite part of the entanglement entropy will scale ‘extensively’ with the law (23) for  $T \gg M$  or the law (20) for  $T \ll M$ . In the cold phase the actual behavior will depend on whether  $\eta_M$  vanishes or not. If  $\eta_M = 0$ , such as the case of resolved walls, the entanglement entropy at very large  $\ell$  makes a  $\mathcal{O}(N_{\text{eff}})$  jump across the thermal phase transition. On the other hand, for soft or hard walls with  $\eta_M \sim 1$  the large- $\ell$  entropy is extensive at *both* low and high temperatures and only the numerical coefficient, proportional to  $\eta_M$ , may jump discontinuously across the deconfining phase transition.

## 4 A cold case example

The characteristic example of an extensive renormalized geometric entropy is that of a highly thermalized state, which is modeled by a large AdS black hole in the holographic map. In this picture, the condition for extensivity is the occurrence of an effective wall at  $u = u_0$  which saturates the growth of the minimal hypersurface as  $\ell \rightarrow \infty$ . In the zero-temperature limit,  $u_0 \sim T \rightarrow 0$  and the extensive term vanishes. In this section we present an example of a system that maintains the extensivity down to zero temperature, provided

we have a magnetic field and/or electric charge densities on the vacuum, supported by a large number of degrees of freedom.

As an explicit example with specific interest we can focus on the extremal dyonic black hole in AdS<sub>4</sub>, studied recently in [17]. This black hole has a zero-temperature horizon with finite entropy density, supported by magnetic and electric fluxes. The holographic dual corresponds to a maximally supersymmetric conformal field theory in 2 + 1 dimensions, the worldvolume theory of a stack of  $N$  M2-branes, in the presence of an external magnetic field and an electric charge chemical potential, both of them associated to a gauged  $U(1)$  subgroup of the  $SO(8)$  R-symmetry. The dyonic black hole is a solution of the Einstein–Maxwell theory on AdS<sub>4</sub> emerging as a consistent truncation of eleven dimensional supergravity on AdS<sub>4</sub> × S<sup>7</sup> [18].

The geometry is given by

$$ds^2 = R^2 u^2 (h(u)d\tau^2 + dx_1^2 + dx_2^2) + \frac{R^2 du^2}{u^2 h(u)}, \quad (25)$$

with

$$h(u) = 1 + (h^2 + q^2)\frac{u_0^4}{u^4} - (1 + h^2 + q^2)\frac{u_0^3}{u^3}, \quad (26)$$

and electromagnetic field

$$F = B dx_1 \wedge dx_2 + \mu u_0 dt \wedge du^{-1}, \quad (27)$$

where the dimensionless electric and magnetic parameters  $h, q$  are related to the magnetic field  $B$  and the charge chemical potential  $\mu$  in the dual CFT by the relations

$$B = h u_0^2, \quad \mu = -q u_0. \quad (28)$$

The Hawking temperature of this black hole is given by

$$T = \frac{u_0}{4\pi} (3 - h^2 - q^2). \quad (29)$$

The crucial property for our purposes is that these black holes admit a zero-temperature limit at finite  $u_0$ , provided  $h^2 + q^2 \rightarrow 3$ . Note that the restriction  $h^2 + q^2 = 3$  is perfectly compatible with general independent values of  $\mu$  and  $B$ . In this limit, the horizon position becomes a function of the magnetic field and the chemical potential through

$$u_0^2 \equiv M_{\text{eff}}^2 = \frac{1}{6} \left[ \mu^2 + \sqrt{\mu^4 + 12B^2} \right]. \quad (30)$$

The resulting model satisfies the conditions laid down in the previous section. There is an effective mass scale determined by the charge and magnetic condensate,  $M_{\text{eff}}$ , which marks the threshold separating the conformal behavior of the entropy,

$$s_A \sim N_{\text{eff}} \left( \frac{1}{\varepsilon} - \frac{1}{\ell} \right) \quad (31)$$

from the extensive behavior

$$s_A \sim N_{\text{eff}} \left( \frac{1}{\varepsilon} + M_{\text{eff}}^2 \ell \right) . \quad (32)$$

One can check the preceding statements by calculating numerically the entanglement entropy per unit length in the direction parallel to the strip. More precisely we find <sup>7</sup>

$$s_A = \frac{\sqrt{2}}{3} N^{\frac{3}{2}} \left\{ \frac{1}{\varepsilon} + f(\ell) \right\} , \quad (33)$$

where  $f(\ell)$  is cutoff independent and interpolates between the two extreme limits (31) and (32), as shown in Fig. 5. The explicit form of  $f(\ell)$  is given parametrically by

$$f(u_*) = u_* \left\{ -1 + \int_0^1 dv \left( \frac{1}{v^2 \sqrt{h(v)} \sqrt{1-v^4}} - \frac{1}{v^2} \right) \right\} , \quad \ell(u_*) = \frac{2}{u_*} \int_0^1 \frac{v^2 dv}{\sqrt{h(v)} \sqrt{1-v^4}} \quad (34)$$

where

$$h(v) = 1 + 3 \frac{u_0^4}{u_*^4} v^4 - 4 \frac{u_0^3}{u_*^3} v^3 .$$

These results can be generalized to arbitrary CFTs in dimension  $d + 1$ , with ‘cold’ charge condensates dual to extremal charged black holes in  $\text{AdS}_{d+2}$  (magnetic fields appear together with the charge only for  $d + 2 = 4$ ). The corresponding supergravity solutions are studied in Ref. [19]. In these cases, the large volume asymptotics of the geometric entropy is controlled by the chemical potential:

$$S_A \sim N_{\text{eff}} M_{\text{eff}}^d |A| , \quad (35)$$

with  $M_{\text{eff}} = \mu$ .

In the preceding discussion we saw how the radius of the black hole vanishes as  $B$  and  $\mu$  are taken to zero, Eq. (30). Therefore, the entanglement entropy  $s_A(\ell, \mu)$  at fixed  $\ell$  also interpolates smoothly between the two asymptotic laws (31) and (32) as  $\mu$  is turned on. One may wonder whether this smooth transition is maintained in other situations, in particular in the case where the CFT lives on a sphere  $S^d$  of radius  $R_S$ , dual to asymptotic AdS geometries in global coordinates [19]. The main effect of the finite radius is to set a minimal value of chemical potential,  $\mu_c \sim 1/R_S$ , below which no extremal black holes are found. This transition is smooth in the sense that the black hole, present for  $\mu > \mu_c$ , still grows from *zero size*, according to the formula

$$u_0(\mu) = M_{\text{eff}} = \frac{\sqrt{d^2 - 1}}{(d + 1)R_S} \sqrt{\frac{\mu^2}{\mu_c^2} - 1} ,$$

---

<sup>7</sup>The absolute normalization follows from the relation  $G_4 = 3R^2/\sqrt{8N^3}$  which gives us in this case  $N_{\text{eff}} = \sqrt{2N^3}/3$ .

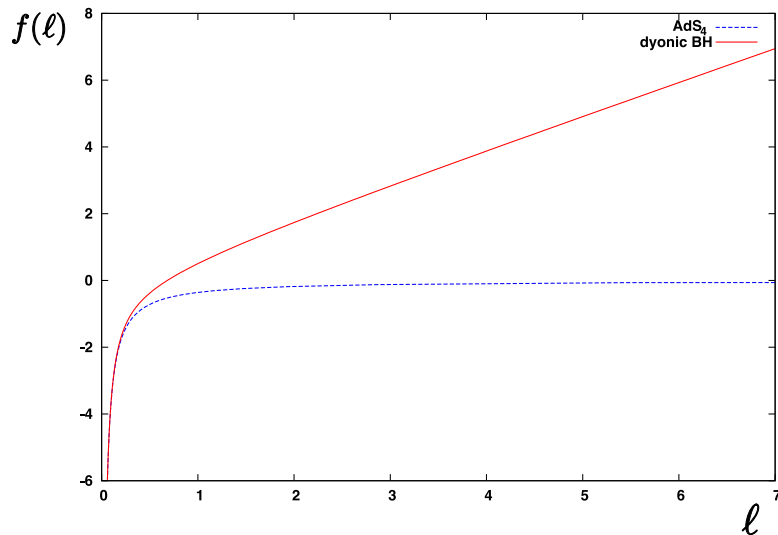


**Figure 5:** Numerical plot of the function  $f(\ell)$ , as defined in Eq. (33), in units where  $u_0 = M_{\text{eff}} = 1$ . The red continuous line corresponds to the case of a CFT in  $2 + 1$  dimensions in the presence of an external magnetic field and/or charge condensate, with a bulk dual given by the dyonic black hole background. The blue dashed line corresponds to the same CFT without any magnetic field or charge condensate, as given by the  $\text{AdS}_4$  dual background. We see how extensive behavior, linear in  $\ell$ , sets in at  $M_{\text{eff}}\ell \gg 1$  in the presence of magnetic field and/or charge condensate.



where  $\mu_c^2 = d/(d-1)R_S^2$ . The phase transition between pure AdS and charged black holes becomes more severe as soon as we depart from zero temperature. Switching on the temperature parameter we generate a critical line in the  $(T, \mu)$  plane,

$$\left(\frac{T}{T_c}\right)^2 + \left(\frac{\mu}{\mu_c}\right)^2 = 1, \quad (36)$$

interpolating between our smooth  $\mu = \mu_c$  critical point at  $T = 0$  and the standard  $\mu = 0$  Hawking–Page transition [20] at  $T = T_c = d/2\pi R_S$ . All  $T > 0$  phase transitions on the critical line (36) are of first order, i.e. as we increase  $\mu$  at fixed  $T$ , the black hole nucleates with a *finite* size  $u_0(T) = 2\pi T/d$ . Hence, a discontinuous behavior of  $s_A$  as a function of  $\mu$  will only occur at  $T > 0$ , at least within the classical approximation, to order  $\mathcal{O}(N_{\text{eff}})$ .

## 5 Concluding remarks

Our main observation in this note is the recognition of the extensivity as a generic property of renormalized entanglement entropy at zero temperature, when calculated using the AdS/CFT ansatz of Ref. [3]. Whenever the holographic geometry shows an infrared ‘wall’ that effectively puts an end to the spacetime, the very large volume asymptotics of the geometric entropy shows extensive behavior *in principle*. In practice, many IR walls in concrete holographic models are associated to vanishing cycles in extra dimensions. In all these cases, as explicitly pointed out in [6], the extensive term in the entropy vanishes to leading order in the  $1/N_{\text{eff}}$  expansion (this was characterized in the text as  $\eta_M = 0$ ). It was suggested in [6] that the vanishing of the renormalized entanglement entropy can be regarded as an order parameter for confinement, as all of these models hold that property. Confinement, or finite string tension, arises in a rather similar fashion from the geometrical point of view, namely the saturation of Wilson loops at an IR wall is very similar to the saturation of minimal hypersurfaces of [3]. There are subtle differences though, since Wilson loops are orthogonal to vanishing cycles in extra dimensions, directly responsible for  $\eta_M = 0$ . On the other hand, in high-temperature plasma phases the extensive behavior of the minimal hypersurfaces resembles that of *spatial* Wilson loops.

In the better-defined models, namely the resolved walls and the thermal walls, one can say that the extensivity is associated to the breaking of conformal symmetry without the generation of a mass gap, since the plasma has  $\mathcal{O}(N_{\text{eff}})$  massless degrees of freedom while, in contrast, the resolved walls have a mass gap and the extensive term in the entropy vanishes.

It is worth stressing that these comments only apply to leading order in the large  $N_{\text{eff}}$  expansion. There are many examples of confinement models *without* strict mass gap, having Goldstone bosons in the spectrum from some spontaneously broken global symmetry (cf. for example [21]). However, in all these cases, the number of massless modes is  $\mathcal{O}(1)$  in the large  $N_{\text{eff}}$  limit, and thus their effects are invisible in the classical approximation to the geometric entropy that is being used here.

The typical example of extensive renormalized entanglement entropy is that of highly thermalized states. We have shown in this paper that one can find systems where the extensivity holds down to zero temperature, supported by magnetic field and/or charge condensates. This is an interesting prediction of the AdS/CFT ansatz for entanglement entropy, although the microscopic interpretation of this property in weak coupling remains an open problem. Indeed, it would be very interesting to check the conditions for this extensivity using purely QFT methods. Finally, the identification of systems with peculiar entropy behavior at zero temperature opens up possible applications to the emerging field of quantum phase transitions [22].

### Acknowledgments

We are indebted to J. I. Cirac, C. Gómez and S. Sachdev for discussions. This work was partially supported by MEC and FEDER under grant FPA2006-05485, CAM under grant HEPHACOS P-ESP-00346 and the European Union Marie Curie RTN network under contract MRTN-CT-2004-005104. C.A.F. enjoys a FPU fellowship from MEC under grant AP2005-0134.

## References

- [1] J. M. Maldacena, “The large N limit of superconformal field theories and supergravity,” *Adv. Theor. Math. Phys.* **2**, 231 (1998) [*Int. J. Theor. Phys.* **38**, 1113 (1999)] [arXiv:hep-th/9711200].  
S. S. Gubser, I. R. Klebanov and A. M. Polyakov, “Gauge theory correlators from non-critical string theory,” *Phys. Lett. B* **428**, 105 (1998) [arXiv:hep-th/9802109].  
E. Witten, “Anti-de Sitter space and holography,” *Adv. Theor. Math. Phys.* **2**, 253 (1998) [arXiv:hep-th/9802150].
- [2] L. Bombelli, R. K. Koul, J. H. Lee and R. D. Sorkin, “A Quantum Source of Entropy for Black Holes,” *Phys. Rev. D* **34**, 373 (1986).  
M. Srednicki, “Entropy and area,” *Phys. Rev. Lett.* **71**, 666 (1993) [arXiv:hep-th/9303048].  
P. Calabrese and J. L. Cardy, “Entanglement entropy and quantum field theory: A non-technical introduction,” *Int. J. Quant. Inf.* **4**, 429 (2006) [arXiv:quant-ph/0505193].
- [3] S. Ryu and T. Takayanagi, “Holographic derivation of entanglement entropy from AdS/CFT,” *Phys. Rev. Lett.* **96**, 181602 (2006) [arXiv:hep-th/0603001].  
“Aspects of holographic entanglement entropy,” *JHEP* **0608**, 045 (2006) [arXiv:hep-th/0605073].
- [4] R. Emparan, “Black hole entropy as entanglement entropy: A holographic derivation,” *JHEP* **0606**, 012 (2006) [arXiv:hep-th/0603081].

- S. Solodukhin, “Entanglement entropy of black holes and AdS/CFT correspondence,” *Phys. Rev. Lett.* **97** 201601 (2006) [arXiv:hep-th/0606205].
- T. Hirata and T. Takayanagi, “AdS/CFT and strong subadditivity of entanglement entropy,” *JHEP* **0702**, 042 (2007) [arXiv:hep-th/0608213].
- V. E. Hubeny, M. Rangamani and T. Takayanagi, “A covariant holographic entanglement entropy proposal,” *JHEP* **0707**, 062 (2007) [arXiv:0705.0016 [hep-th]].
- V. E. Hubeny and M. Rangamani, “Holographic entanglement entropy for disconnected regions,” arXiv:0711.4118 [hep-th].
- [5] G. Vidal, J. I. Latorre, E. Rico and A. Kitaev, “Entanglement in quantum critical phenomena,” *Phys. Rev. Lett.* **90**, 227902 (2003) [arXiv:quant-ph/0211074].
- [6] I. R. Klebanov, D. Kutasov and A. Murugan, “Entanglement as a Probe of Confinement,” arXiv:0709.2140 [hep-th].
- [7] T. Nishioka and T. Takayanagi, “AdS bubbles, entropy and closed string tachyons,” *JHEP* **0701**, 090 (2007) [arXiv:hep-th/0611035].
- [8] H. Casini and M. Huerta, “A finite entanglement entropy and the c-theorem,” *Phys. Lett. B* **600** (2004) 142 [arXiv:hep-th/0405111].
- H. Casini, C. D. Fosco and M. Huerta, “Entanglement and alpha entropies for a massive Dirac field in two dimensions,” *J. Stat. Mech.* **0507** (2005) P007 [arXiv:cond-mat/0505563].
- H. Casini and M. Huerta, “Entanglement and alpha entropies for a massive scalar field in two dimensions,” *J. Stat. Mech.* **0512** (2005) P012 [arXiv:cond-mat/0511014].
- [9] P. Calabrese and J. L. Cardy, “Entanglement entropy and quantum field theory,” *J. Stat. Mech.* **0406** (2004) P002 [arXiv:hep-th/0405152].
- [10] N. R. Constable and R. C. Myers, “Exotic scalar states in the AdS/CFT correspondence,” *JHEP* **9911**, 020 (1999) [arXiv:hep-th/9905081].
- A. Kehagias and K. Sfetsos, “On asymptotic freedom and confinement from type-IIB supergravity,” *Phys. Lett. B* **456**, 22 (1999) [arXiv:hep-th/9903109].
- S. S. Gubser, “Dilaton-driven confinement,” arXiv:hep-th/9902155.
- [11] J. Polchinski and M. J. Strassler, “Hard scattering and gauge/string duality,” *Phys. Rev. Lett.* **88**, 031601 (2002) [arXiv:hep-th/0109174].
- [12] P. Kraus, F. Larsen and S. P. Trivedi, “The Coulomb branch of gauge theory from rotating branes,” *JHEP* **9903**, 003 (1999) [arXiv:hep-th/9811120].
- [13] D. J. Gross and H. Ooguri, “Aspects of large N gauge theory dynamics as seen by string theory,” *Phys. Rev. D* **58**, 106002 (1998) [arXiv:hep-th/9805129].

- [14] M. Nielsen and I. Chuang, *Quantum Computation and Quantum Information*, Cambridge University Press, 2000.
- [15] M. M. Wolf, F. Verstraete, M. B. Hastings and J. I. Cirac, “Area laws in quantum systems: mutual information and correlations,” *Phys. Rev. Lett.* **100**, 070502 (2008) [arXiv:0704.3906 [quant-ph]].
- [16] A. Faraggi, L. A. Pando Zayas and C. A. Terrero-Escalante, “Holographic Entanglement Entropy and Phase Transitions at Finite Temperature,” arXiv:0710.5483 [hep-th].
- [17] S. A. Hartnoll and P. Kovtun, “Hall conductivity from dyonic black holes,” *Phys. Rev. D* **76**, 066001 (2007) [arXiv:0704.1160 [hep-th]].  
S. A. Hartnoll, P. K. Kovtun, M. Muller and S. Sachdev, “Theory of the Nernst effect near quantum phase transitions in condensed matter, and in dyonic black holes,” *Phys. Rev. B* **76** (2007) 144502 [arXiv:0706.3215 [cond-mat.str-el]].
- [18] C. P. Herzog, P. Kovtun, S. Sachdev and D. T. Son, “Quantum critical transport, duality, and M-theory,” *Phys. Rev. D* **75** (2007) 085020 [arXiv:hep-th/0701036].
- [19] A. Chamblin, R. Emparan, C. V. Johnson and R. C. Myers, “Charged AdS black holes and catastrophic holography,” *Phys. Rev. D* **60**, 064018 (1999) [arXiv:hep-th/9902170].
- [20] S. W. Hawking and D. N. Page, “Thermodynamics Of Black Holes In Anti-De Sitter Space,” *Commun. Math. Phys.* **87**, 577 (1983).  
E. Witten, “Anti-de Sitter space, thermal phase transition, and confinement in gauge theories,” *Adv. Theor. Math. Phys.* **2**, 505 (1998) [arXiv:hep-th/9803131].
- [21] S. S. Gubser, C. P. Herzog and I. R. Klebanov, “Symmetry breaking and axionic strings in the warped deformed conifold,” *JHEP* **0409** (2004) 036 [arXiv:hep-th/0405282].
- [22] S. Sachdev, *Quantum Phase Transitions*, Cambridge University Press, Cambridge (1999).